Copyright © 2000, by the author(s).
All rights reserved.

Permission to make digital or hard copies of all or part of this work for personal or classroom use is granted without fee provided that copies are not made or distributed for profit or commercial advantage and that copies bear this notice and the full citation on the first page. To copy otherwise, to republish, to post on servers or to redistribute to lists, requires prior specific permission.

AN OXYGEN DISCHARGE MODEL FOR A LARGE AREA PLASMA SOURCE (LAPS)

by

Kazushige Takechi and M. A. Lieberman

Memorandum No. UCB/ERL M00/33

22 June 2000

AN OXYGEN DISCHARGE MODEL FOR A LARGE AREA PLASMA SOURCE (LAPS)

by

Kazushige Takechi and M. A. Lieberman

Memorandum No. UCB/ERL M00/33

22 June 2000

ELECTRONICS RESEARCH LABORATORY

College of Engineering
University of California, Berkeley
94720

An Oxygen Discharge Model for a Large Area Plasma Source (LAPS)

Kazushige Takechi[1] and M. A. Lieberman[2]

[1]*Visiting Industrial Fellow, NEC Corporation in Japan*
[2]*Department of Electrical Engineering and Computer Sciences*
University of California at Berkeley
Berkeley, CA 94720

ABSTRACT

We develop a simplified oxygen discharge model corresponding to our large area plasma source (LAPS) geometry. For a given gas pressure and absorbed power, we solve the particle and energy balance equations with proper boundary conditions in two dimensions in order to determine the electron temperature, ion and oxygen atom density profiles, and their fluxes to the substrate holder. With the incorporation of an electron-neutral particle ionization term into the diffusion equation, we investigate the effect of the ionization near the plasma edge on the plasma density profiles. We find that, with increasing gas pressure, the plasma density profile becomes steeper in the middle and flatter at the metal chamber wall, and the ionization zone is limited to smaller annular regions surrounding the antenna quartz tubes. For the fluxes, we find that, with increasing pressure, the flux of oxygen atoms lost to the substrate holder increases whereas that of oxygen ions incident on it decreases.

1. Introduction

In a previous letter, we reported on the first operation of an inductively coupled large area plasma source (LAPS) driven by a 13.56 MHz traveling wave with oxygen gas.[1] We plan to do some photoresist etching experiments on the LAPS with an oxygen plasma. In the etch processes, ion and O-atom fluxes at the substrate surface are crucial variables. These fluxes must be found using an oxygen discharge model which accounts for the generation of both etchant atoms (O atoms) and bombarding ions.

We describe a simplified oxygen discharge model corresponding to the LAPS in a simplified two-dimensional geometry. For a given gas pressure and absorbed power, we solve the particle and energy balance equations with proper boundary conditions in order to determine the electron temperature, ion and oxygen atom density profiles, and their fluxes to the substrate holder.

2. Model formulation

Our oxygen discharge model is based on the particle and energy balance in the discharge. The ionized particles generated in the plasma as well as the associated energy input must be equal to the particle and energy losses in the volume and through particle diffusion to the reactor walls.[2] A finite element analysis is performed in two dimensions for the LAPS chamber. Due to symmetry of the chamber, only one quarter (x:30 cm $\times$ y:10 cm $\times$ z:35 cm) of the chamber is included in the analysis (Fig. 1).

Assumptions of our model are listed below.

(1) Steady state is assumed.

(2) For simplicity, we ignore negative ions. We thus take $n = n_i = n_e$, where n is the plasma density, n_i is the positive ion density, and n_e is the electron density.

(3) We take into account the following two reactions for the ionization and dissociation processes.[2,3]

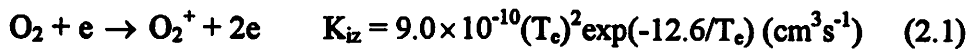

$$O_2 + e \rightarrow O_2^+ + 2e \qquad K_{iz} = 9.0\times10^{-10}(T_e)^2\exp(-12.6/T_e)\ (cm^3s^{-1}) \qquad (2.1)$$

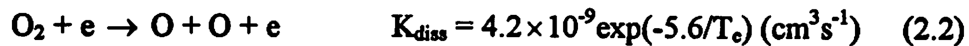

$$O_2 + e \rightarrow O + O + e \qquad K_{diss} = 4.2\times10^{-9}\exp(-5.6/T_e)\ (cm^3s^{-1}) \qquad (2.2)$$

where K_{iz} is the ionization rate constant, K_{diss} is the dissociation rate constant, and T_e is the electron temperature.

(4) The ion loss velocity is the Bohm velocity $u_B = (eT_e/M)^{1/2}$.

(5) The ion temperature T_i and O-atom temperature T_o are assumed to be 0.05 V for gas pressures ranging from 1 mTorr (gas density : 3.3×10^{13} cm^{-3}) to 100 mTorr (gas density : 3.3×10^{15} cm^{-3}).

Ion particle balance is obtained from the diffusion equation (2.3)

$$\nabla^2 n(x,y) + n(x,y)\frac{K_{iz}}{D_a} n_{O_2} \sum_{i=1}^{8} \exp\left(\frac{R - r_i(x,y)}{\lambda_{iz(O_2)}}\right) = 0 \quad (2.3)$$

where $n(x,y) = n_i(x,y) = n_e(x,y)$ is the plasma density profile, $D_a = (T_e/T_i)^{1/2} u_B / n_{O2}\sigma_i$ is the ambipolar diffusion coefficient, n_{O2} is the gas density, and K_{iz} is the ionization rate constant. To investigate the effect of the ionization near the plasma edge on the plasma density profiles, we incorporate an electron-neutral particle ionization term (exponential term), where R is the radius of the quartz tubes, $r_i(x,y)$ is the distance from the center of each quartz tube, and λ_{iz} is the electron-neutral particle ionization length. In argon discharges, the pressure dependence of λ_{iz} is given approximately by[4)]

$$\lambda_{iz(Ar)}(cm) = \frac{125}{p(mTorr)} \quad (2.4)$$

Since λ_{iz} is proportional to σ_{iz}^{-1} (ionization cross section) and the maximum σ_{iz} is proportional to ε_{iz}^{-2} (ε_{iz}: ionization energy)[2)], we use the following scaling

$$\lambda_{iz(O_2)} = \lambda_{iz(Ar)} \times \left(\frac{12.6}{15.76}\right)^2 = \frac{80}{p(mTorr)} \quad (2.5)$$

The boundary conditions for equation (2.3) are

$$\nabla n(x,y)\,|_{walls} = -\frac{u_B}{D_a} n(x,y) \quad (2.6)$$

$$\nabla n(x,y)\,|_{plasma} = 0 \quad (2.7)$$

where the subscript "walls" means the substrate holder metal, side metal, and quartz, and the "plasma" means the plasma boundary of the calculation area, as shown in Fig. 1.

Partial differential equation (2.3) is solved numerically using the Finite Element Method for eigenvalue problems. Since u_B and D_a are functions of T_e, we need a value of T_e to solve the equation (2.3). Assuming an initial value of T_{e0}, we solve the equation (2.3) to obtain a solution n(x,y) and eigenvalue. With given D_a and n_{O2}, the eigenvalue gives K_{iz}. We then compare the obtained K_{iz} with our initial K_{iz0} which is estimated by substituting the initial T_{e0} into equation (2.1). We iterate our solution until the K_{iz} given by the eigenvalue becomes reasonably close to our initial estimate K_{iz0}, indicating that the plasma parameters are found within the accuracy of the calculation. This procedure gives numerical values for the electron temperature T_e and plasma density profile n(x,y), depending on the gas density n_{O2}. It should be noted that n(x,y) gives the plasma density profile and does not give information on the absolute magnitude of the density. The latter is obtained from energy balance

considerations.

Using the electron temperature T_e and plasma density profile n(x,y), we solve another diffusion equation (2.8).

$$-D_O \nabla^2 n_O(x,y) = 2K_{diss}(T_e) n(x,y) n_{O_2} \quad (2.8)$$

Equation (2.8) expresses the O-atom particle balance, where D_O is the diffusion coefficient for O atoms due to collisions with O_2 molecules, $n_O(x,y)$ is the O-atom density profile, and $K_{diss}(T_e)$ is the dissociation coefficient as defined in (2.2). The diffusion coefficient D_O is

$$D_O = \frac{eT}{M_R \nu_{O,O_2}} \quad (2.9)$$

where M_R is the reduced mass and

$$\nu_{O,O_2} = n_{O_2} \sigma_{O,O_2} \overline{v_{O,O_2}} \quad (2.10)$$

is the collision frequency for a constant cross-section process. Inserting $\nu_{O,O2}$ into D_O yields

$$D_O = \frac{\pi}{8} \lambda_{O,O_2} \overline{v_{O,O_2}} \quad (2.11)$$

where $\lambda_{O,O2} = 1/n_{O2}\sigma_{O,O2}$ is the mean free path.[2] We take the cross section $\sigma_{O,O2} = 3.0 \times 10^{-15}$ cm^2, which is smaller than that ($\sigma_{O2,O2} = 5.0 \times 10^{-15}$ cm^2) for self-diffusion of O_2 molecules due to collisions with O_2 molecules. The boundary conditions for equation (2.8) are

$$\Gamma_{O-metal} = -D_O \nabla n_O(x,y)|_{metal} = \gamma_{metal} \times \frac{1}{4} n_{O-metal}(x,y) \overline{v_O} \quad (2.12)$$

$$\Gamma_{O-quartz} = -D_O \nabla n_O(x,y)|_{quartz} = \gamma_{quartz} \times \frac{1}{4} n_{O-quartz}(x,y) \overline{v_O} \quad (2.13)$$

$$-D_O \nabla n_O(x,y)|_{plasma} = 0 \quad (2.14)$$

where $v_O = (8eT_O/\pi M_O)^{1/2}$, γ_{metal} is the metal-surface recombination coefficient, and γ_{quartz} is the quartz-surface recombination coefficient. We take $\gamma_{metal} = 0.1$, suggesting that one out of every ten O atoms which strike the metal surface will recombine to form O_2. We take $\gamma_{quartz} = 0.0001$ since, for a surface which is passivated with oxygen, the recombination coefficient is considered to be much lower.[3]

Partial differential equation (Poisson's equation) (2.8) is also solved numerically using the Finite Element Method. The solution gives the numerical value for the O-atom density profile $n_O(x,y)$, depending on the plasma density profile n(x,y) and gas density n_{O2}. We note that $n_O(x,y)$ is the O-atom density profile and does not give information on the absolute density.

We next consider the energy balance for oxygen discharges. The collisional energy loss per electron-ion pair created, $E_c(T_e)$, which is a function of the electron temperature, is an important quantity. In oxygen gas, $E_c(T_e)$ can be a factor of 2-10 times higher than for a noble gas (e.g. argon) at the same electron temperature since it includes additional collisional energy losses such as excitation of vibrational and rotational energy and molecular dissociation. In addition to $E_c(T_e)$, electrons and ions carry kinetic energy to the walls. For Maxwellian electrons, the mean kinetic energy lost per electron lost E_e is $2T_e$. The mean kinetic energy lost per ion lost $E_i(T_e)$ can be expressed as

$$E_i = \frac{T_e}{2} + \frac{T_e}{2}\ln\left(\frac{M}{2\pi m}\right) \quad (2.15)$$

where m is the electron mass and M is the ion mass.[2)] In oxygen plasmas, we take $E_i = 5.1T_e$. Summing the three contributions yields the total energy lost per ion lost from the system:

$$E_T = E_c + E_e + E_i = E_c(T_e) + 2T_e + 5.1T_e \quad (2.16)$$

At pressures for which the ion loss velocity is the Bohm velocity u_B, the overall discharge energy balance can be expressed in terms of E_T as

$$P_{abs} = e\int_{walls} E_T \Gamma_i \cdot dS \quad (2.17)$$

where P_{abs} is the power absorbed by the plasma, dS is the area element for particle loss, and Γ_i is the ion flux expressed as

$$\Gamma_i = -D_a \nabla n(x,y)_{walls} = n(x,y)_{walls} u_B = n_{is}(x,y) u_B \quad (2.18)$$

In our system configuration, equation (2.17) can be written as

$$P_{abs} = e\int_{quartz} E_T \Gamma_{i-quartz} \cdot dS + e\int_{subst} E_T \Gamma_{i-subst} \cdot dS + e\int_{side} E_T \Gamma_{i-side} \cdot dS \quad (2.19)$$

The terms on the right-hand side of (2.19) account for the energy loss at the four quartz tube surfaces, at the substrate holder surface, and at the chamber side surface, shown in Fig. 1.

Substituting the solution of equation (2.3) into a set of the equations (2.18) and (2.19) yields the absolute value of the ion flux at each surface. Similarly, from the equations (2.12) and (2.13), we obtain the absolute value of the O-atom flux at each surface. The equations (2.12), (2.13), and (2.18) also give the absolute values of the O-atom density at the surface and the ion density at the plasma-sheath edge.

3. Results and discussion

3-1. Plasma density profiles and O-atom density profiles

We first describe how the electron temperature T_e and plasma density profile n(x,y) change depending on the oxygen gas pressure. Equation (2.3) for ion particle balance is solved with boundary

conditions (2.6) and (2.7) to determine T_e and n(x,y). We note that T_e is determined by particle balance alone, and is independent of the absorbed power.

Figure 2 shows the dependence of electron temperature on gas pressure. As seen in the figure, the variation of electron temperature is similar to that in the literature,[3,5] with T_e decreasing with increasing pressure.

Figures 3, 4, 5, 6, and 7 show the plasma density profiles for oxygen gas pressures of 1, 5, 20, 50, and 100 mTorr, respectively. The z axis in the figures has an arbitrary unit. The density profiles roughly follow a sinusoid pattern in general, which is typical for a diffusion dominated plasma discharge. We see that, as the gas pressure increases, the plasma density profile becomes steeper in the middle and flatter at the metal surfaces, and the ionization zone is limited to smaller annular regions surrounding the quartz tubes. For high pressure regime $p \geq 20$ mTorr, the mean free path of the energetic (ionizing) electrons $\lambda_{iz(O2)}$ is less than the discharge length. In this situation, most of the ionization is performed in the edge regions.

We next describe how the O-atom density profile $n_O(x,y)$ changes depending on the oxygen gas pressure. With the obtained solution n(x,y), equation (2.8) for O-atom particle balance is solved with boundary conditions (2.12), (2.13), and (2.14) to determine $n_O(x,y)$.

Figures 8, 9, 10, 11, and 12 show the O-atom density profiles for oxygen gas pressures of 1, 5, 20, 50, and 100 mTorr, respectively. The z axis in the figures has an arbitrary unit. Since the mean free path $\lambda_{O,O2}$ is less than the characteristic size of the plasma, gas-phase O atoms created within the plasma are transported to the surfaces by diffusion. We see that, as the gas pressure increases, the O-atom density profile becomes steeper in the middle and flatter at the metal surfaces, which has been also seen for the plasma density profile. O atoms are not depleted near the quartz tubes since we take $\gamma_{quartz} = 0.0001$, indicating that almost all the O atoms entering the quartz surfaces leave the surfaces without surface recombination. If we took a higher recombination coefficient, O atoms near the quartz tubes would be depleted through surface recombination to generate O_2 molecules.

We have assumed that one out of every ten O atoms recombines on the substrate holder wall. In fact, depending on the wall and substrate materials, there can be even larger recombination on them.[3,5] To see the situations, we solve the equation (2.8) using different recombination coefficients for the substrate holder wall. Figures 13, 14, and 15 show the O-atom density profiles at the gas pressure of 20 mTorr for $\gamma_{subst\text{-}metal} = 0.1$, 0.5, and 0.9, respectively. For a large $\gamma_{subst\text{-}metal}$, as expected, O atoms near the substrate holder are depleted due to the wall recombination.

3-2. Ion and O-atom fluxes at the substrate holder

With the obtained solution n(x,y), equations (2.18) and (2.19) for energy balance are solved to determine the absolute flux of ions incident on the substrate holder ($\Gamma_{i\text{-}subst}$) and that of O atoms lost to the substrate holder ($\Gamma_{O\text{-}subst}$). We also consider the plasma density (n_{is}) and O-atom density (n_{Os}) at the substrate holder wall. The results presented here are at a fixed absorbed power P_{abs} = 500 W and recombination coefficient $\gamma_{metal} = 0.1$.

Figure 16 shows the flux of ions incident on the substrate holder as a function of the distance from the center of the chamber. We see that, with increasing pressure, $\Gamma_{i\text{-}subst}$ monotonically decreases and becomes more non-uniform over the substrate holder. The non-uniformity at high pressures can be explained by diffusive loss at the wall. In oxygen discharges, as gas pressure increases, E_c greatly increases with decreasing T_e. E_T thus increases with increasing pressure, resulting in the decrease in $\Gamma_{i\text{-}subst}$ from equation (2.17).

We next consider how the absorbed power is distributed to the three surface regions (three terms on the right-hand side of equation (2.19)), depending on the gas pressure. Figure 17 shows the dependence of fractional power distribution on gas pressure. As the gas pressure increases, the power dissipated at the four quartz walls increases while the powers dissipated at the substrate holder wall and chamber side wall decrease. This is due to the fact that, with increasing pressure, most of the ionization occurs in the smaller annular regions surrounding the quartz tubes.

Figure 18 shows the flux of O atoms lost to the substrate holder as a function of the distance from the center of the chamber. With increasing pressure, $\Gamma_{O\text{-}subst}$ greatly increases and becomes more non-uniform over the substrate holder. For $\Gamma_{O\text{-}subst}$, we have a scaling[2)]

$$\Gamma_{O-subst} \propto \frac{P_{abs}}{E_T}\left(\frac{n_{O_2}}{h_l u_B}\right)^{1-\varepsilon_{diss}/\varepsilon_{iz}} \qquad (3.1)$$

where h_l is approximately estimated from equation (3.2)[2)]

$$h_l = \left[1+\left(C\frac{u_B}{D_a}\right)^2\right]^{-1/2} \propto \frac{D_a}{u_B} \propto \frac{1}{u_B n_{O_2}} \qquad (3.2)$$

where C is a constant. From equations (3.1) and (3.2), we obtain

$$\Gamma_{O-subst} \propto \frac{P_{abs}}{E_T}\left(n_{O_2}{}^2\right)^{1-5.6/12.6} = \frac{P_{abs}}{E_T} n_{O_2}{}^{1.11} \qquad (3.3)$$

The scaling (3.3) is in reasonable agreement with the ratio obtained from Fig. 18. As has been seen, with increasing pressure, the flux of ions falls roughly proportional to E_T^{-1}, whereas that of O atoms

considerably increases proportional to $n_{O2}^{1.11}/E_T$.

The ion density at the substrate holder sheath edge (n_{is}) is determined from (2.18) as

$$n_{is} = \frac{\Gamma_{i-subst}}{u_B} \quad (3.4)$$

Figure 19 shows the dependence of n_{is} on the distance from the center of the chamber. The trend is similar to that for $\Gamma_{i-subst}$, with n_{is} decreasing with increase pressure.

The O-atom density at the substrate holder surface (n_{Os}) is determined from (2.12) as

$$n_{Os} = \frac{\Gamma_{O-subst}}{\gamma_{metal} v_O} \quad (3.5)$$

Figure 20 shows the dependence of n_{Os} on the distance from the center of the chamber. The behavior is similar to that for $\Gamma_{O-subst}$, with n_{Os} increasing with increase pressure. Fractional dissociation of the neutral feed gas O_2 is in the range of 0.1 - 0.2 at 500 W. If the absorbed power were higher, a higher degree of dissociation would be achieved. Such high dissociation will result in a high concentration of O atoms which can directly influence process output parameters such as photoresist etch rate.

4. Conclusions

From our simulations, we have found that, with increasing oxygen gas pressure, the plasma density profile and O-atom density profile become steeper in the middle and flatter at the metal chamber wall, and the ionization zone is limited to smaller annular regions surrounding the antenna quartz tubes. The recombination coefficient $\gamma_{subst-metal}$ also influences the O-atom density profile near the substrate holder. For the fluxes, we have found that, with increasing pressure, oxygen ion flux incident on the substrate holder decreases, whereas O-atom flux lost to it increases. For the power dissipation, we have found that, with increasing gas pressure, the power dissipated at the quartz walls increases while the powers dissipated at the substrate holder wall and chamber side wall decrease.

We would like to incorporate the effect on O-atom density of O-atom loss at the substrate due to etch reactions into this model, and compare the model with experimental results for photoresist etch.

References

1) K. Takechi and M. A. Lieberman, Operation of a large area plasma source (LAPS) with oxygen gas, Memorandum UCB/ERL M00/15, Electronics Research Laboratory, University of California, Berkeley, (2000).

2) M. A. Lieberman and A. J. Lichtenberg, *Principles of Plasma Discharges and Materials Processing,*

John Wiley & Sons Inc., 605 Third Avenue, New York, NY, (1994).

3) C. Lee and M. A. Lieberman, Global model of Ar, O_2, Cl_2, and Ar/O_2 high-density plasma discharges, J. Vac. Sci. Technol. A 13(2), 368-380 (1995).

4) V. P. Gopinath and M. A. Lieberman, Simulation and analysis of a large area plasma source, Memorandum UCB/ERL M95/65, Electronics Research Laboratory, University of California, Berkeley, (1995).

5) K. Patel, Volume averaged modeling of high density discharges, Memorandum UCB/ERL M98/28, Electronics Research Laboratory, University of California, Berkeley, (1998).

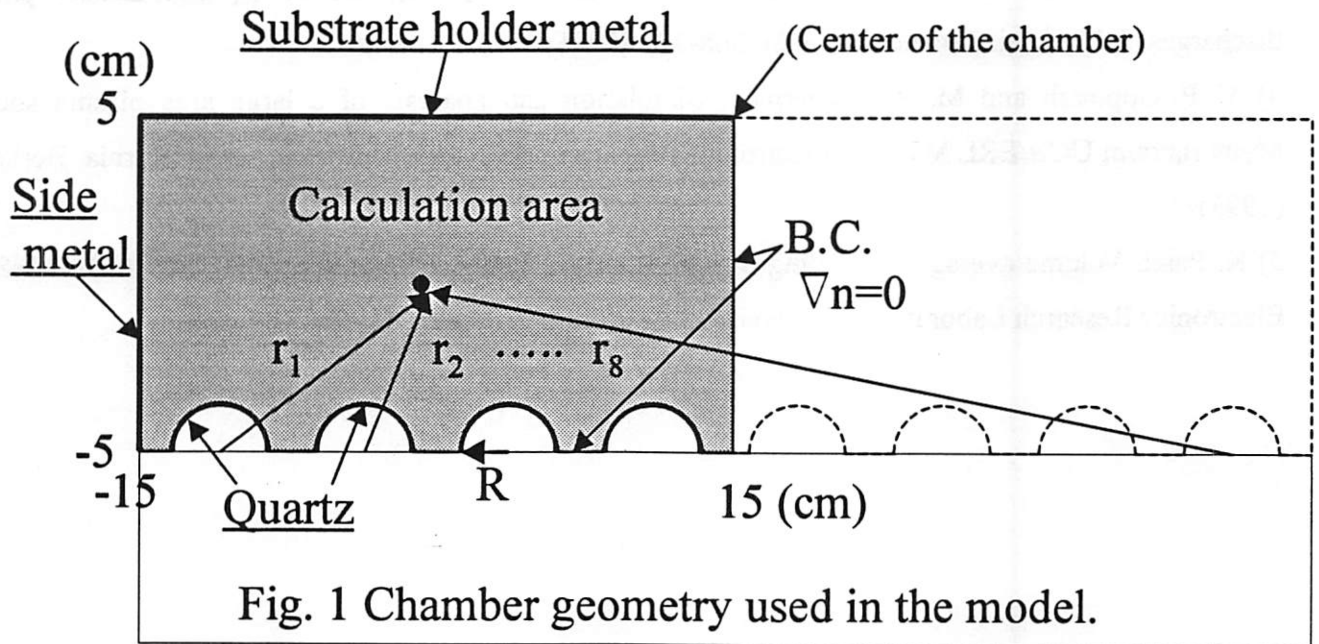

Fig. 1 Chamber geometry used in the model.

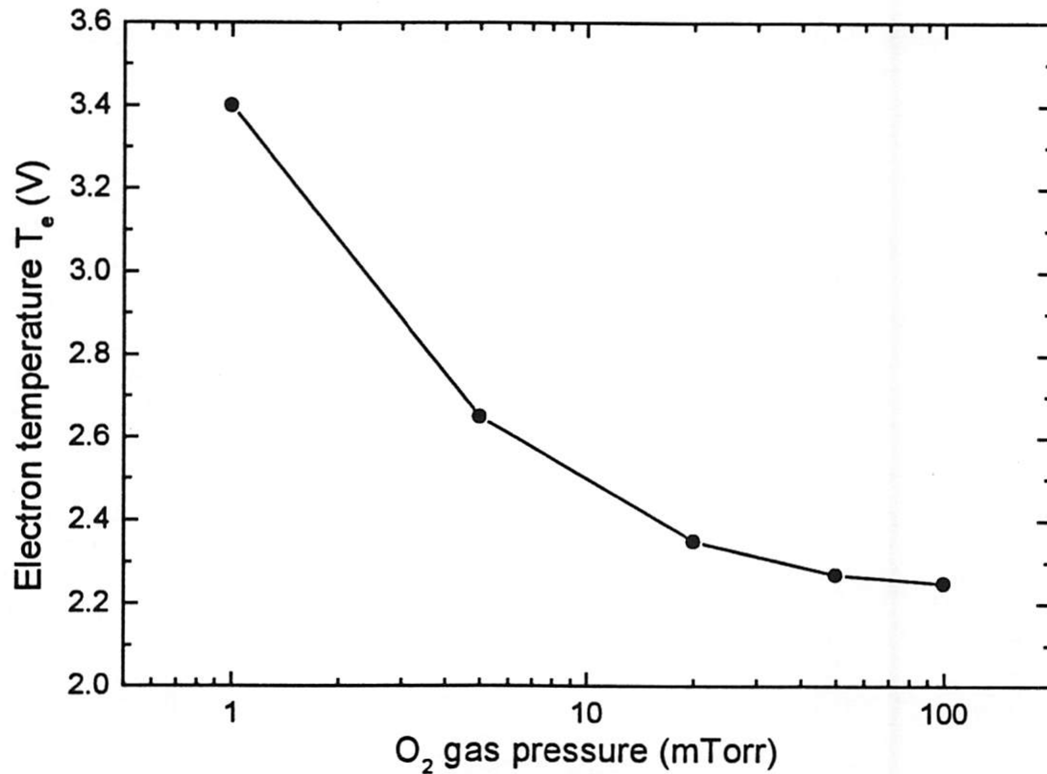

Fig. 2 Electron temperature vs gas pressure for O_2 discharge.

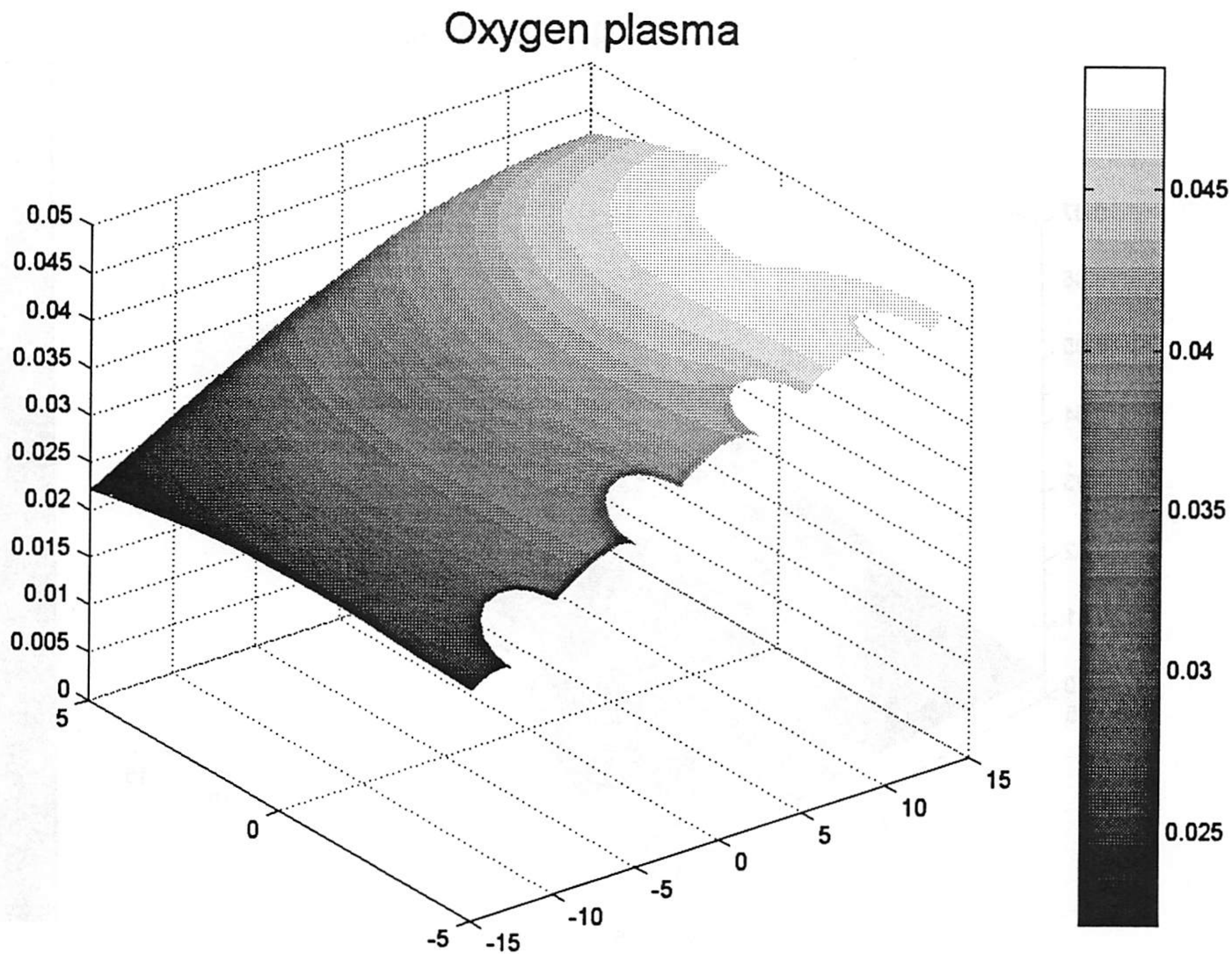

Fig. 3 Plasma density profile for p = 1 mTorr.

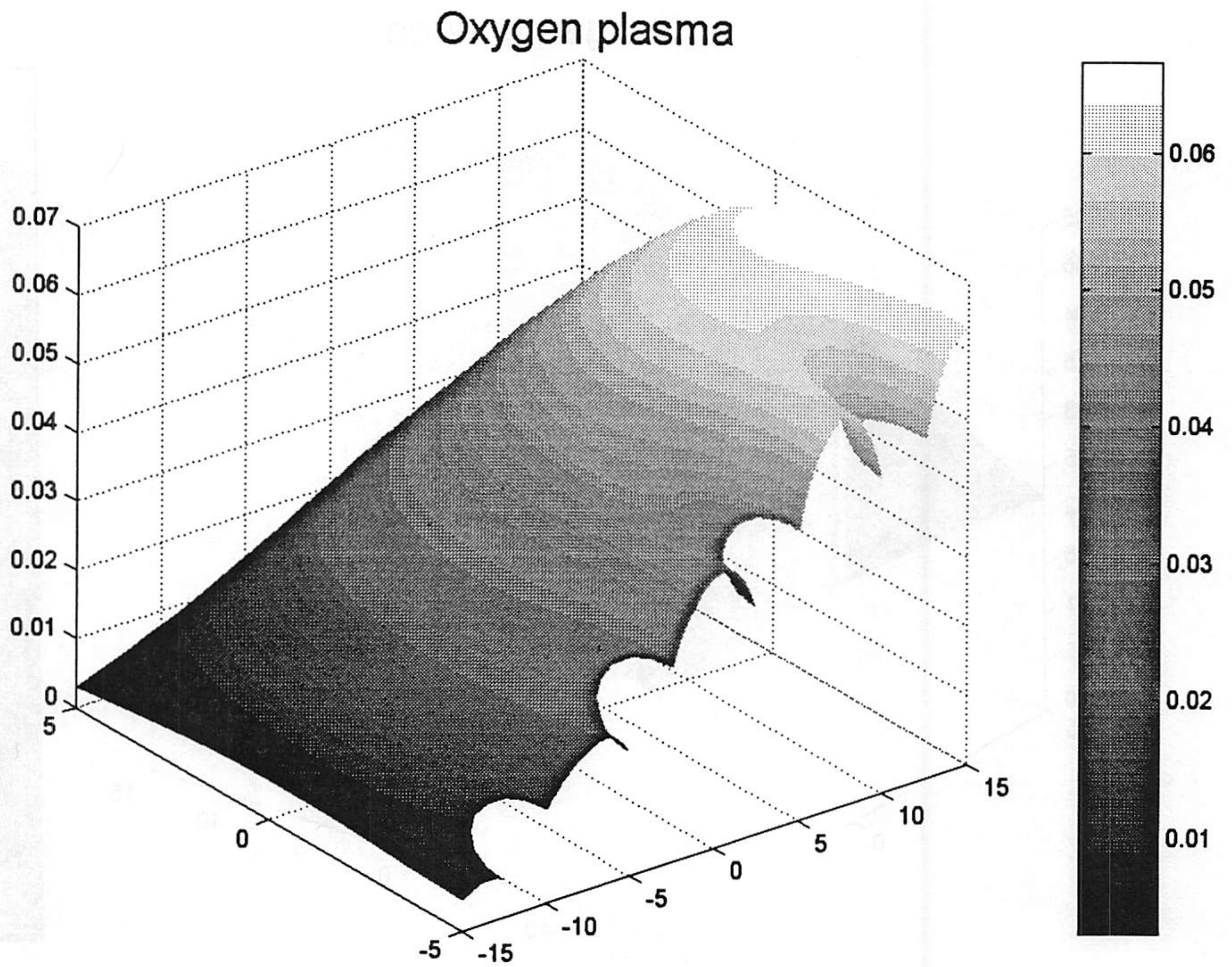

Fig. 4 Plasma density profile for p = 5 mTorr.

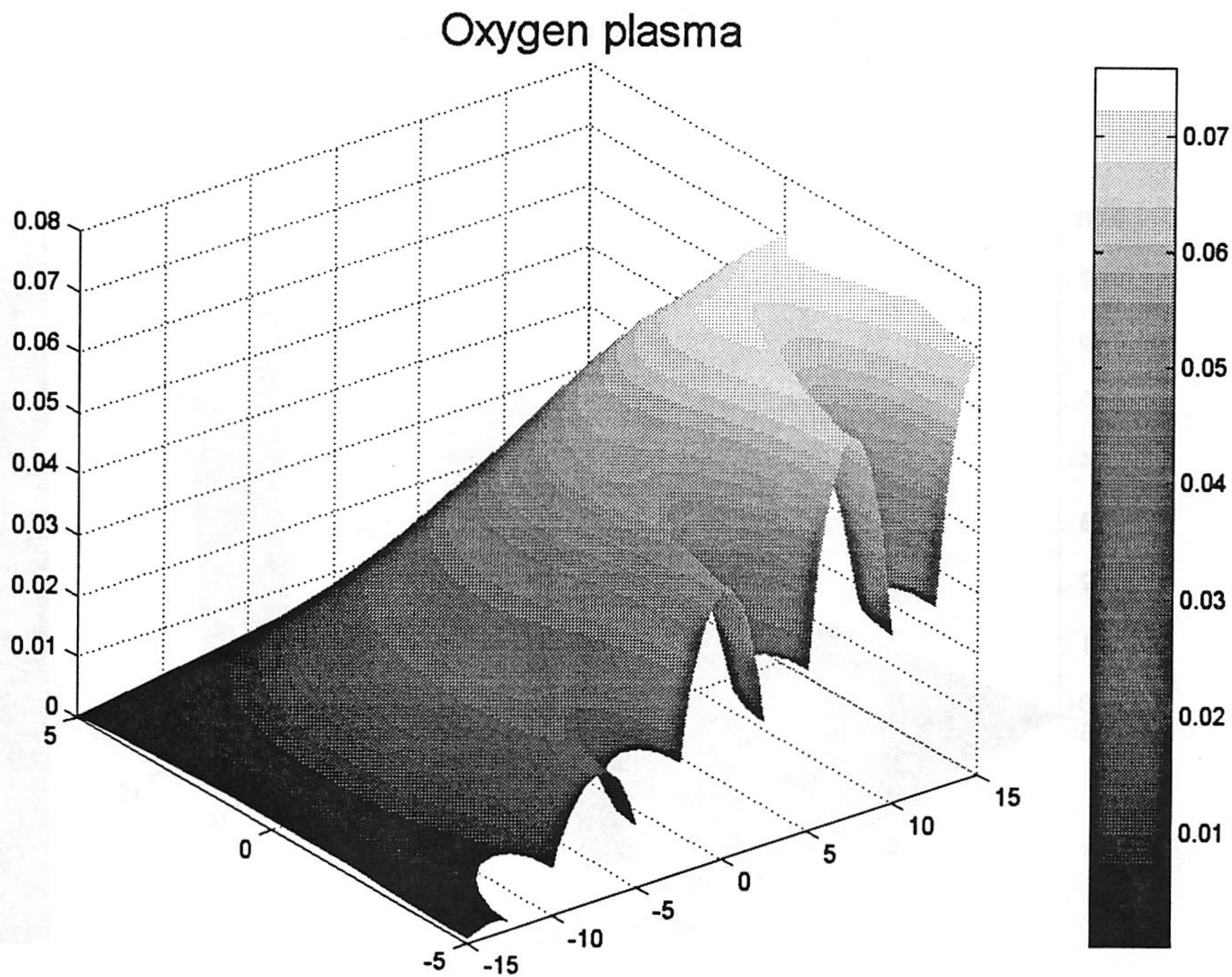

Fig. 5 Plasma density profile for p = 20 mTorr.

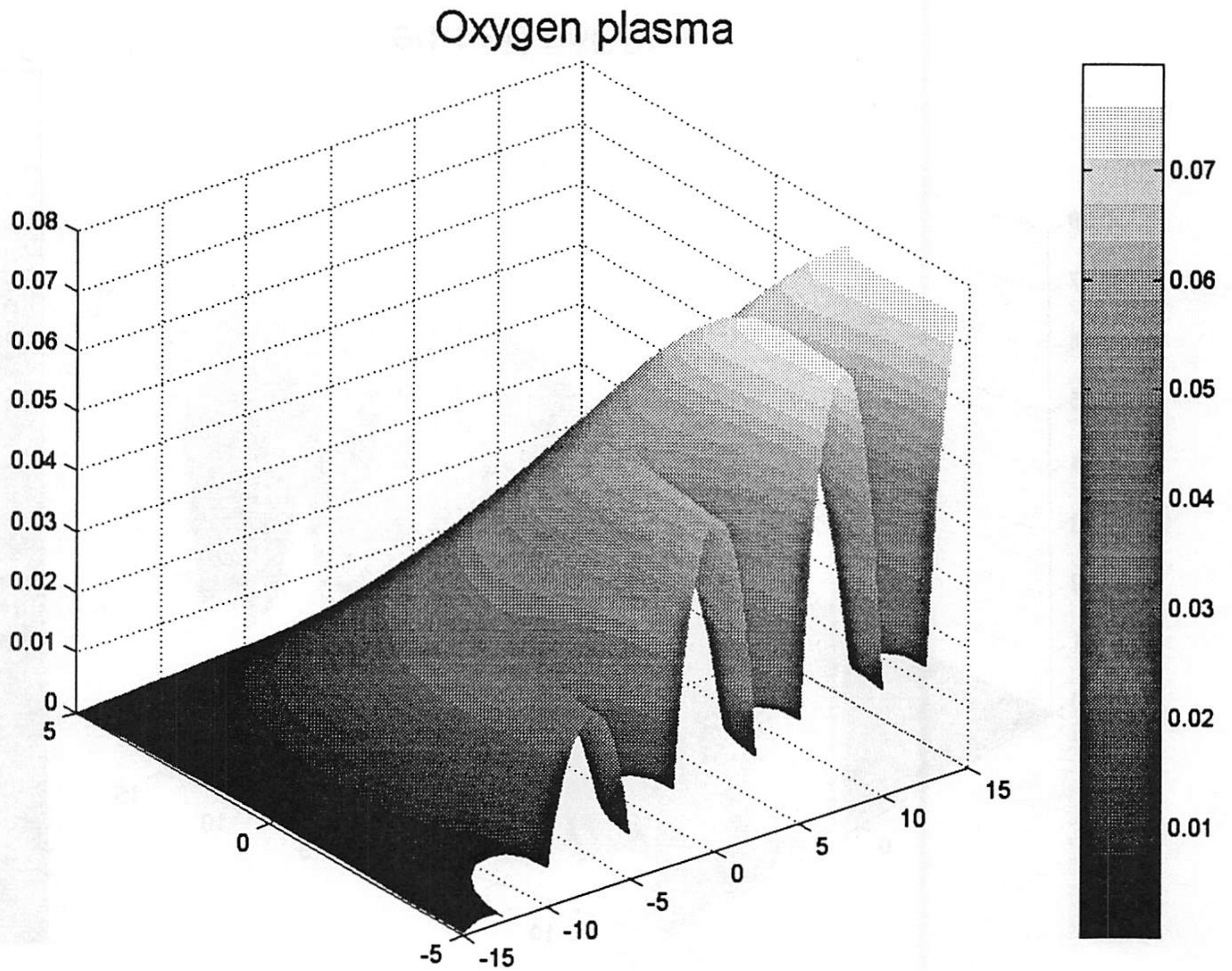

Fig. 6 Plasma density profile for p = 50 mTorr.

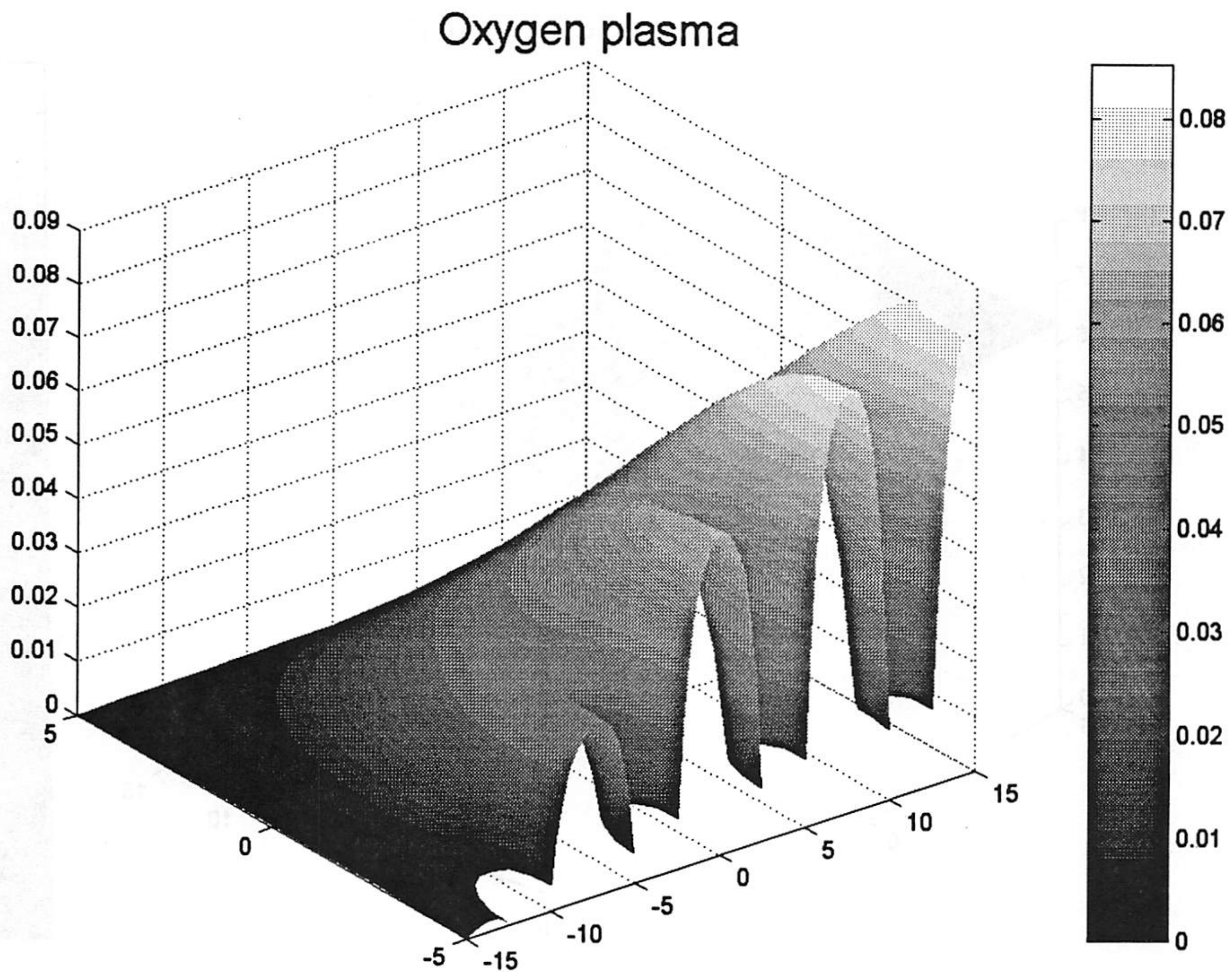

Fig. 7 Plasma density profile for p = 100 mTorr.

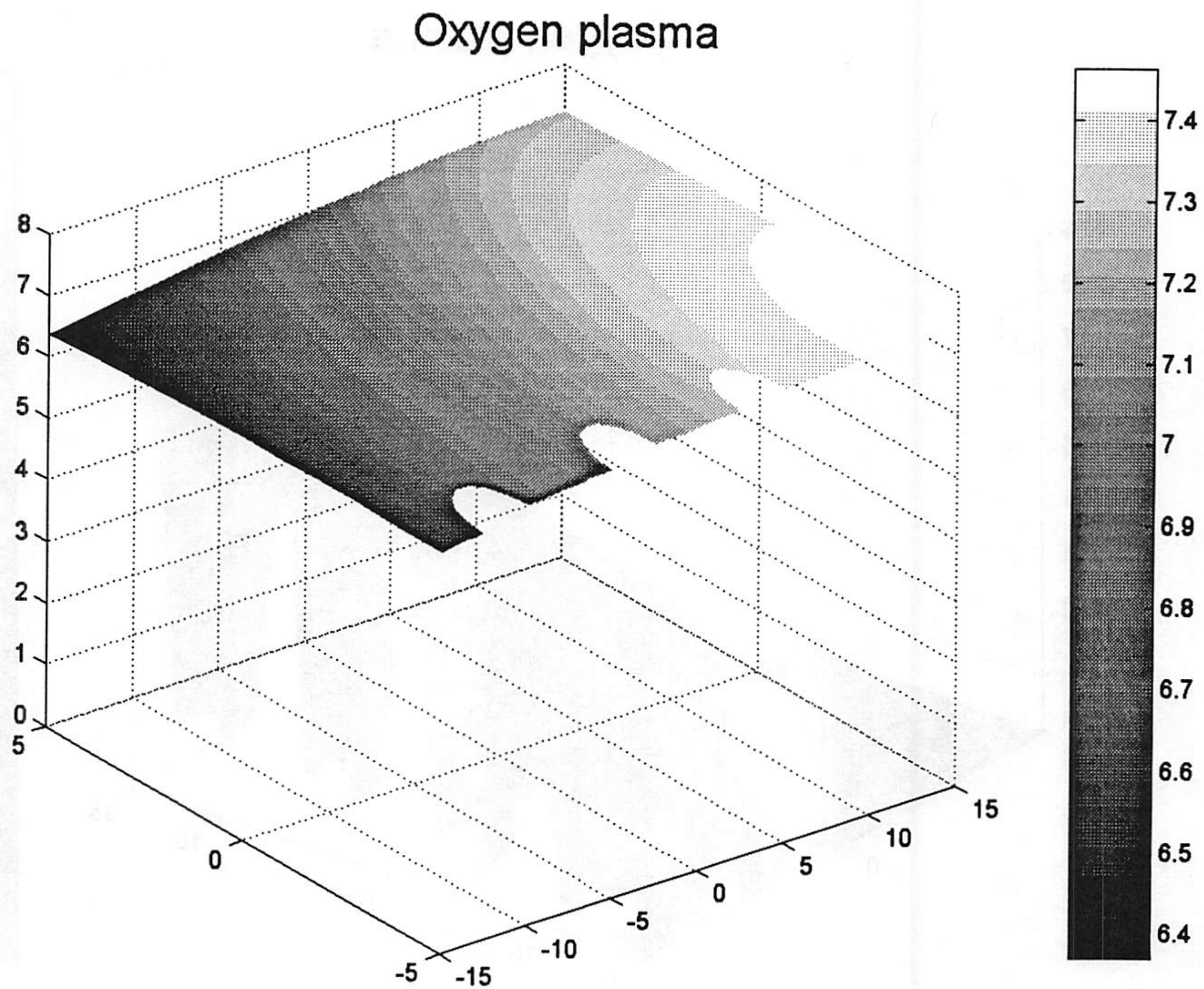

Fig. 8 O-atom density profile for p = 1 mTorr.

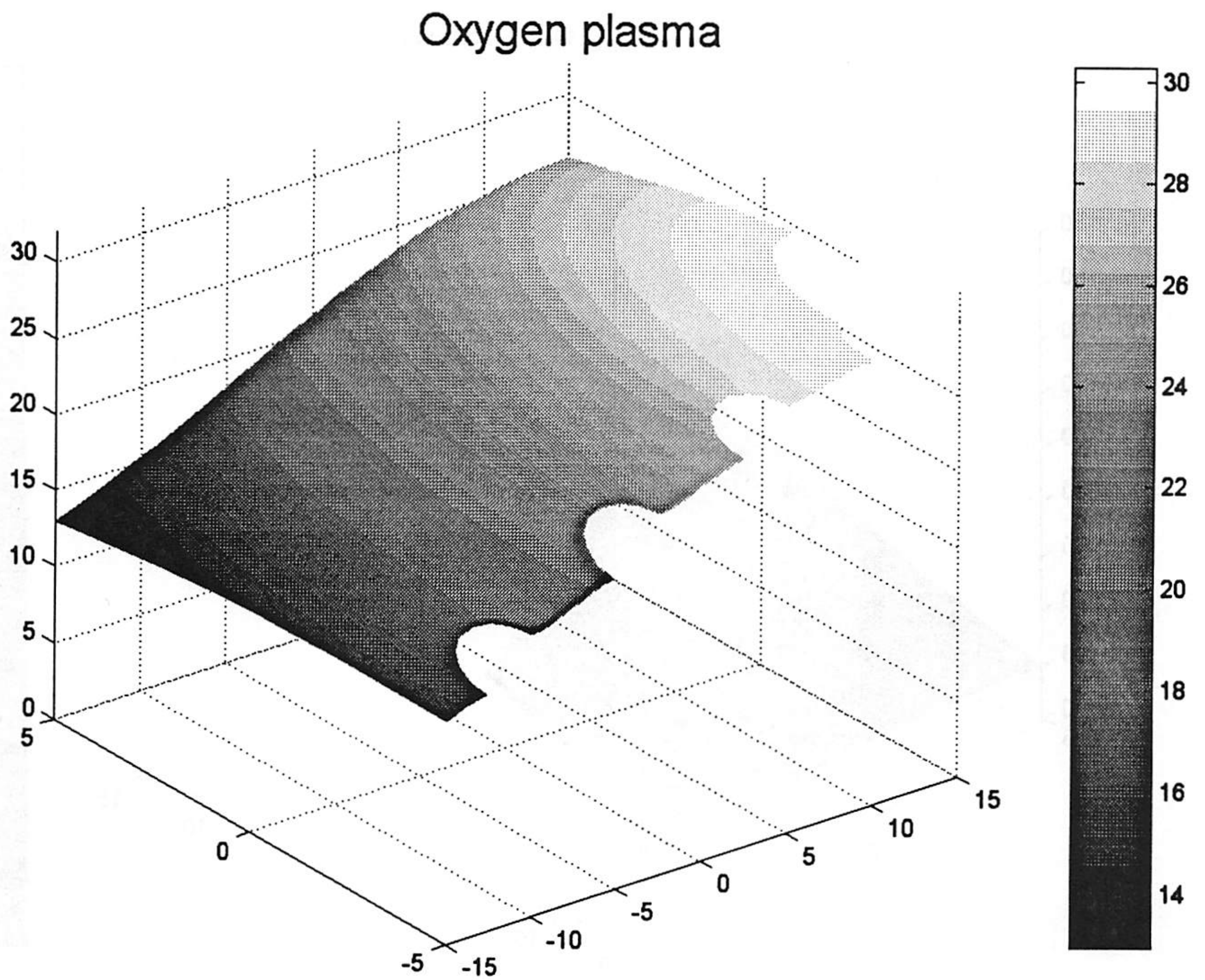

Fig. 9 O-atom density profile for p = 5 mTorr.

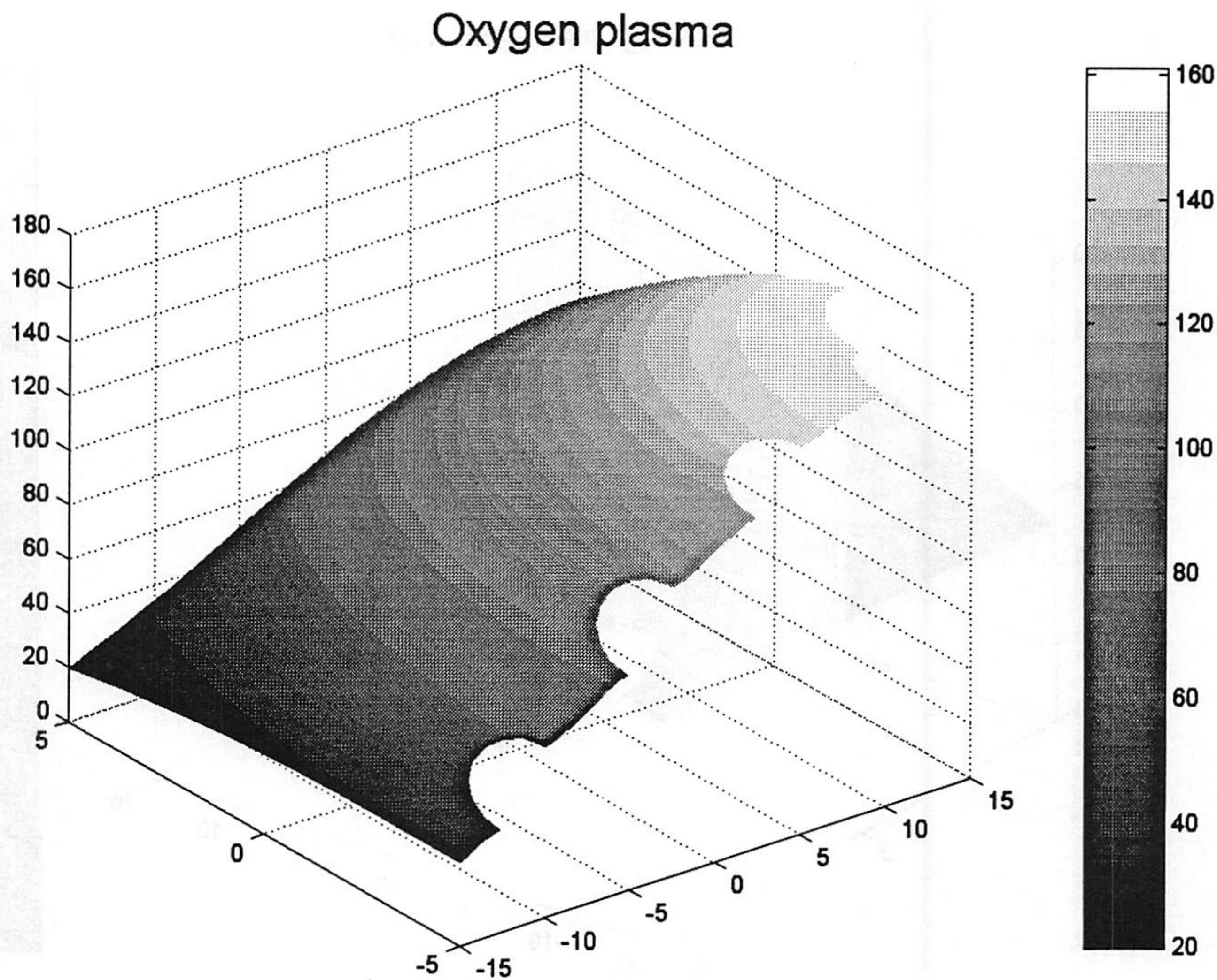

Fig. 10 O-atom density profile for p = 20 mTorr.

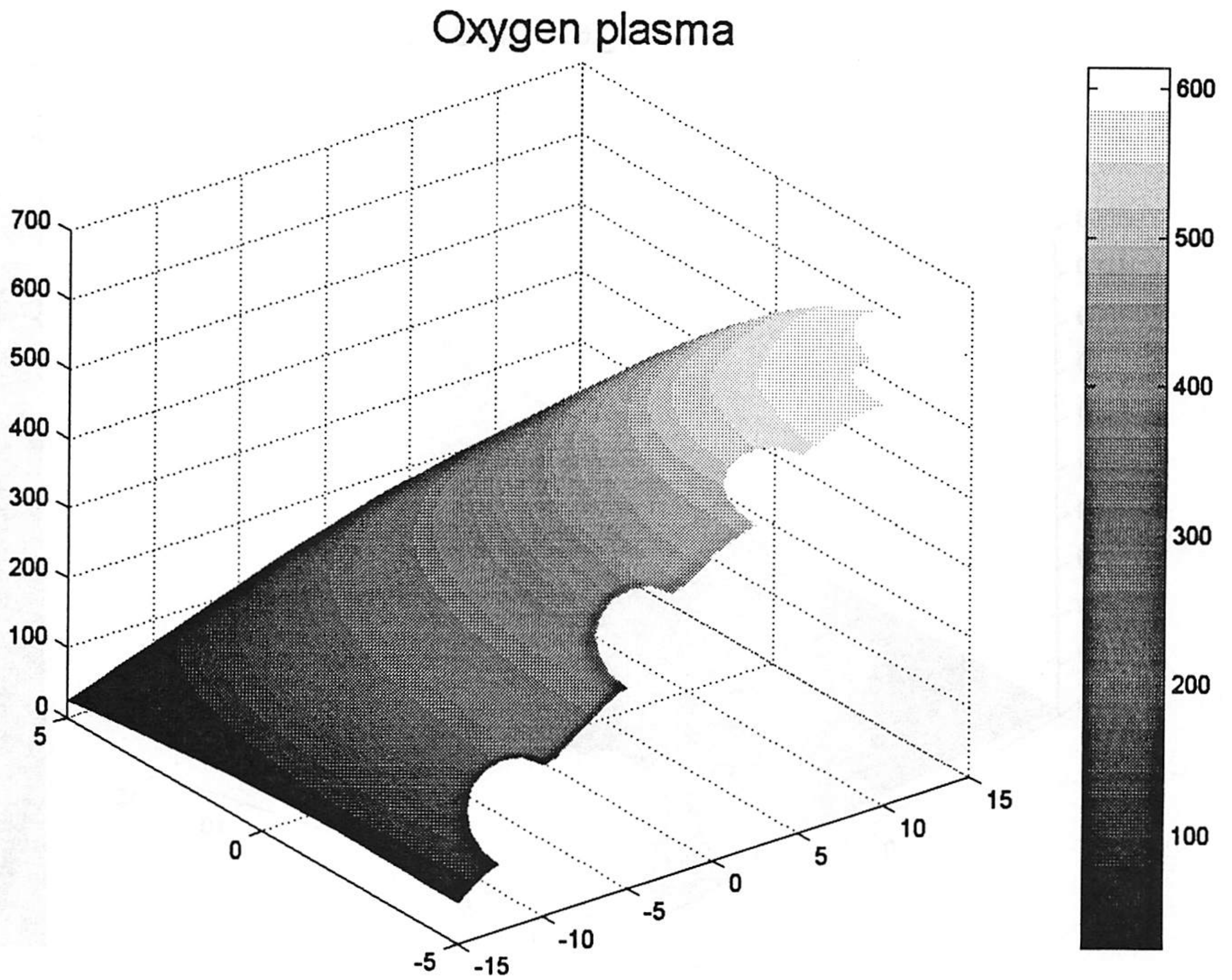

Fig. 11 O-atom density profile for p = 50 mTorr.

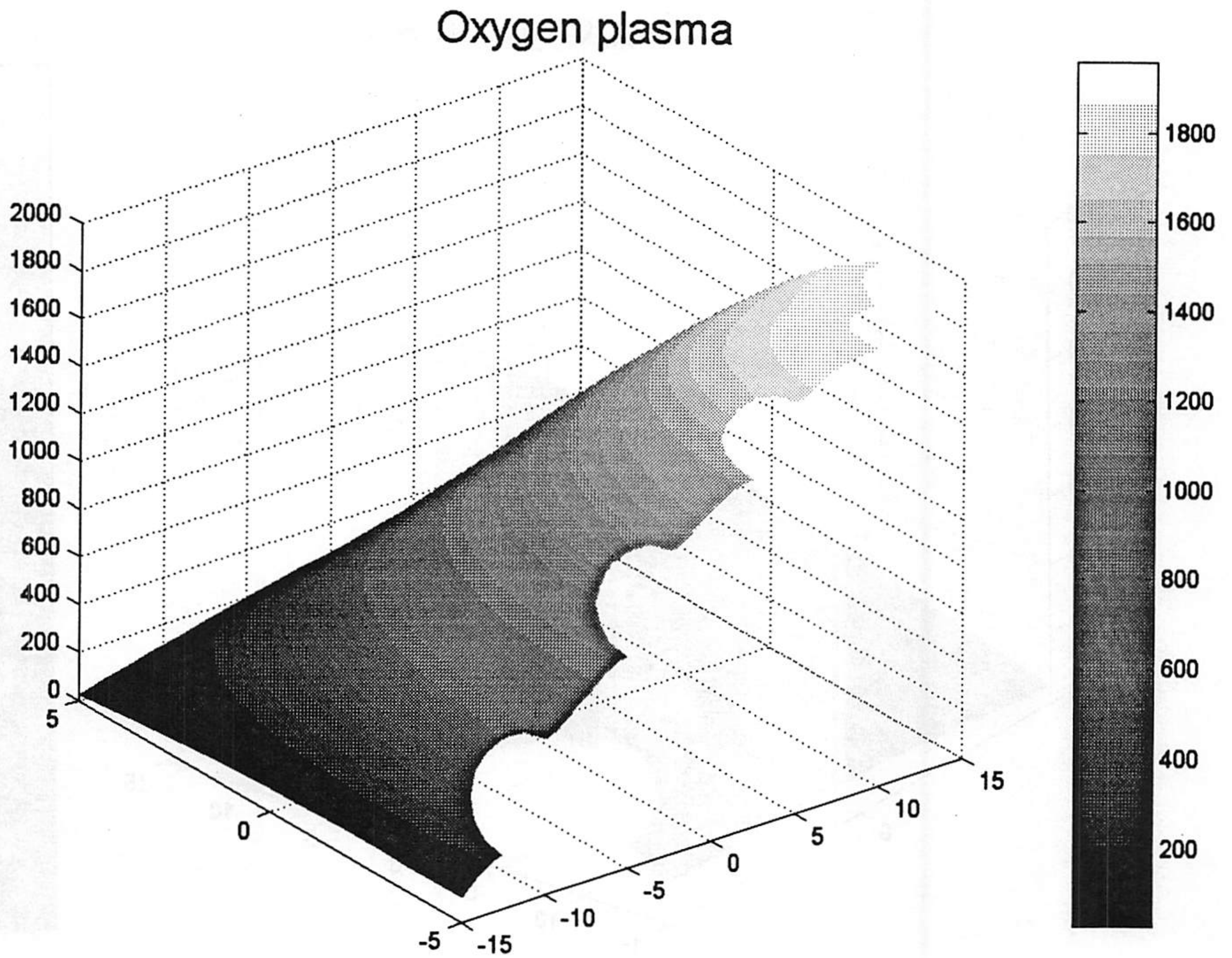

Fig. 12 O-atom density profile for p = 100 mTorr.

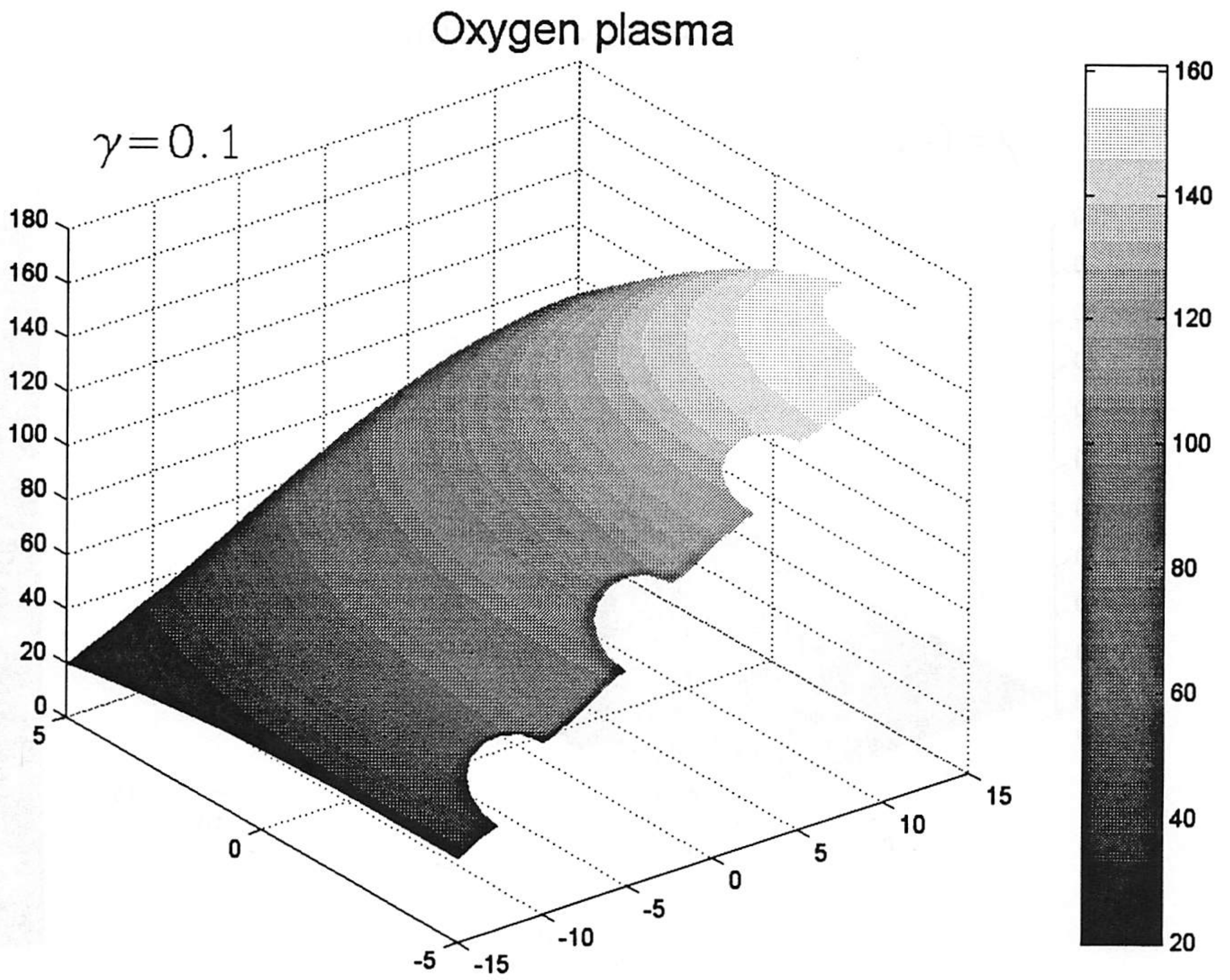

Fig. 13 O-atom density profile for p = 20 mTorr.

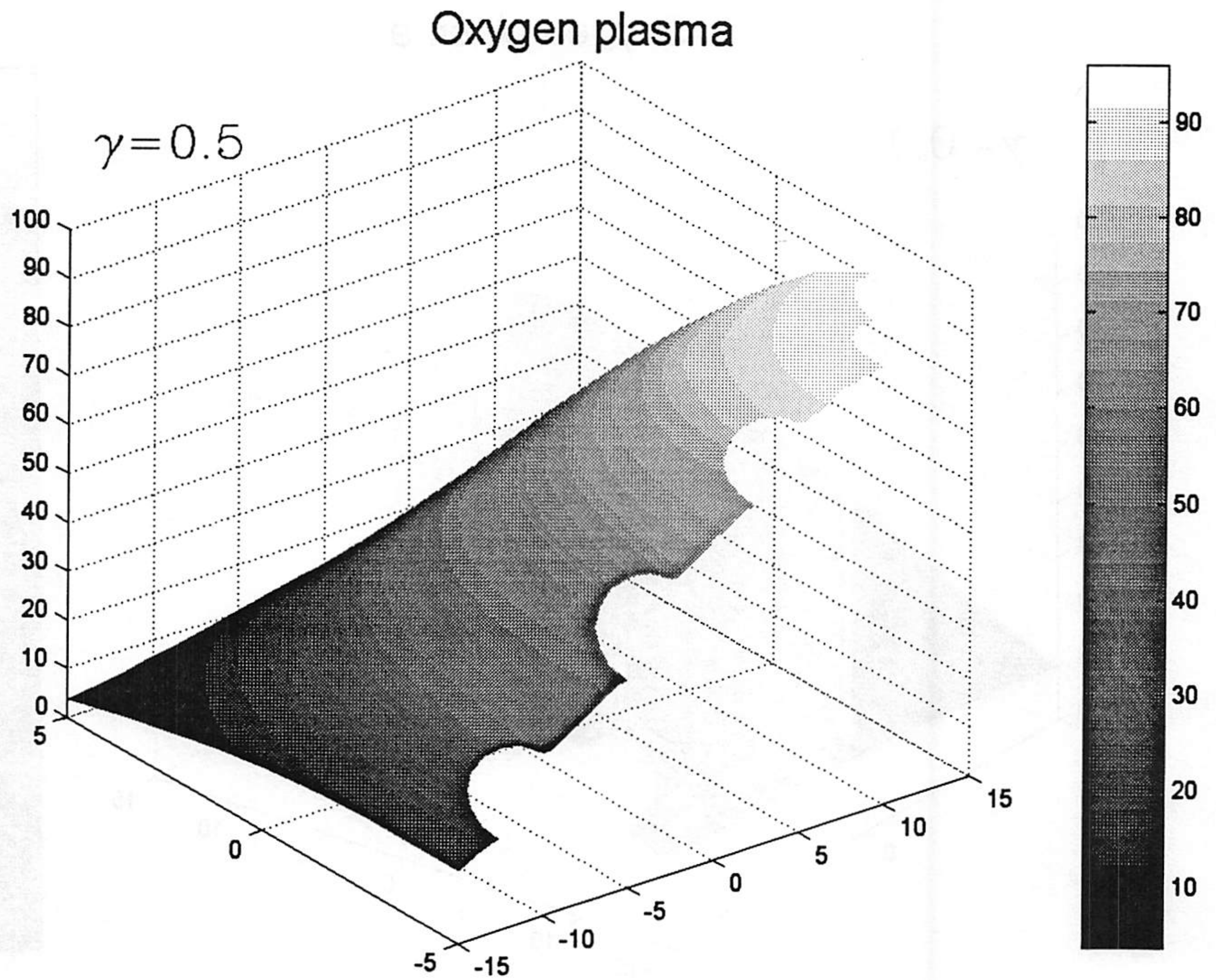

Fig. 14 O-atom density profile for p = 20 mTorr.

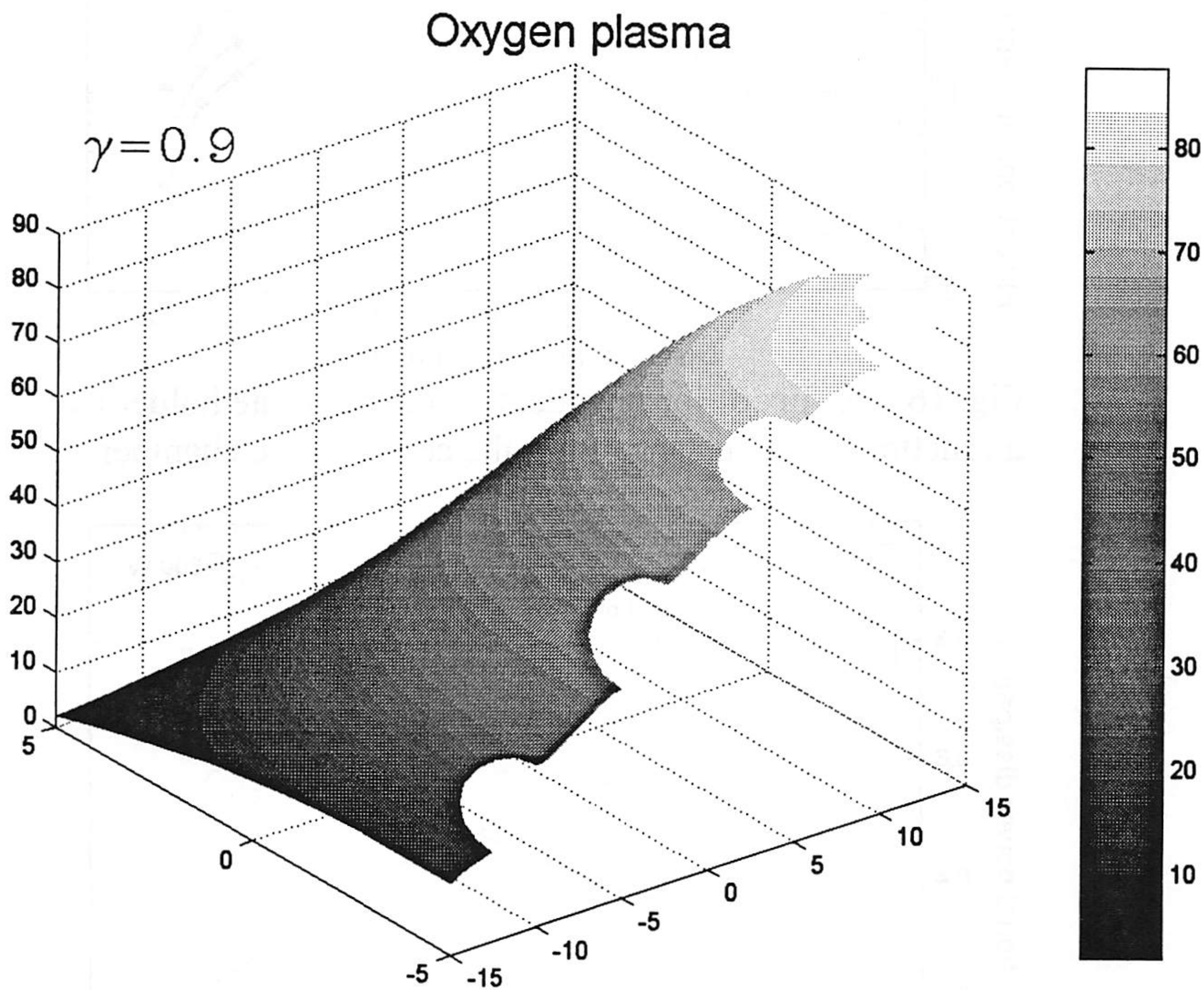

Fig. 15 O-atom density profile for p = 20 mTorr.

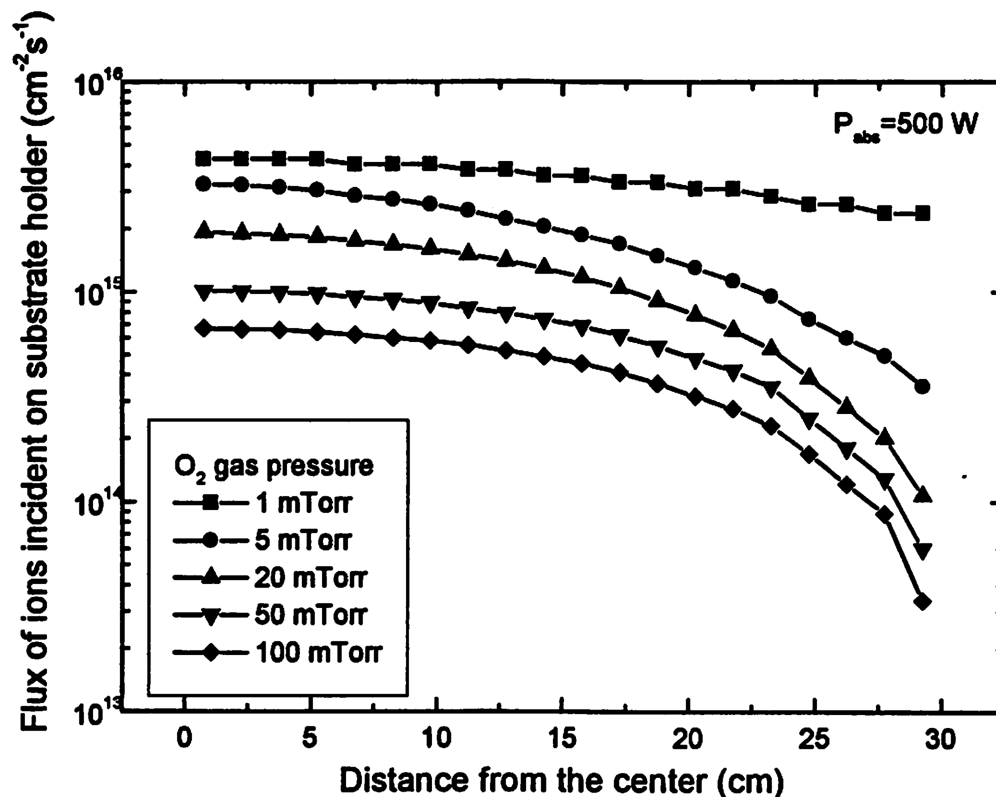

Fig. 16 The flux of ions incident on the substrate holder as a function of the distance from the center of the chamber.

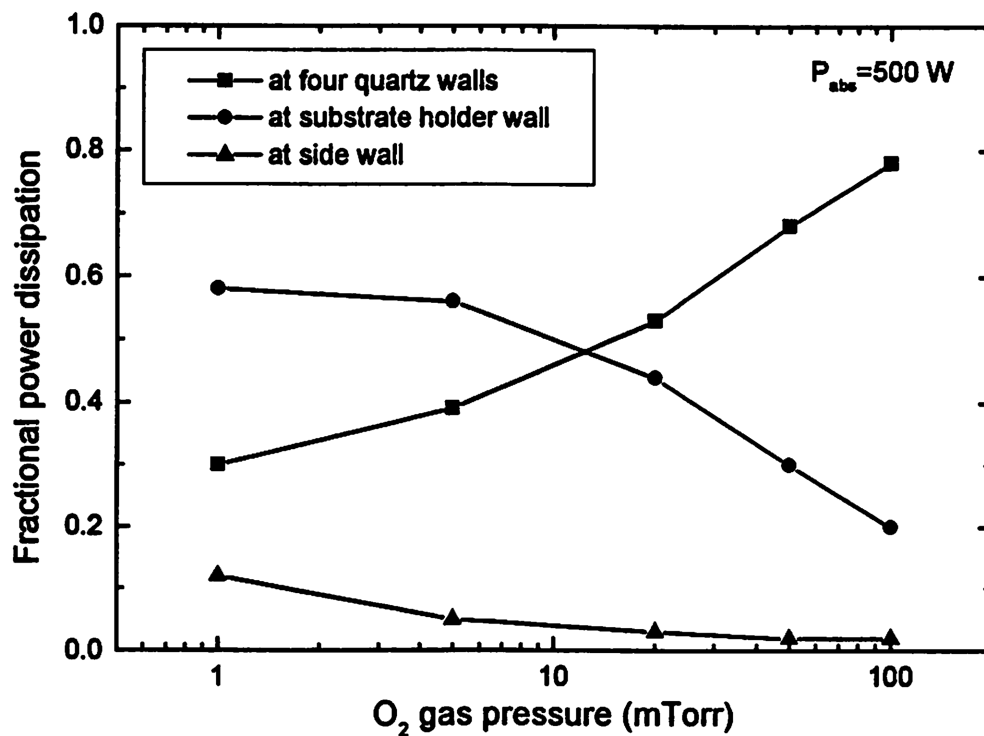

Fig. 17 Dependence of the fractional power dissipation on the gas pressure.

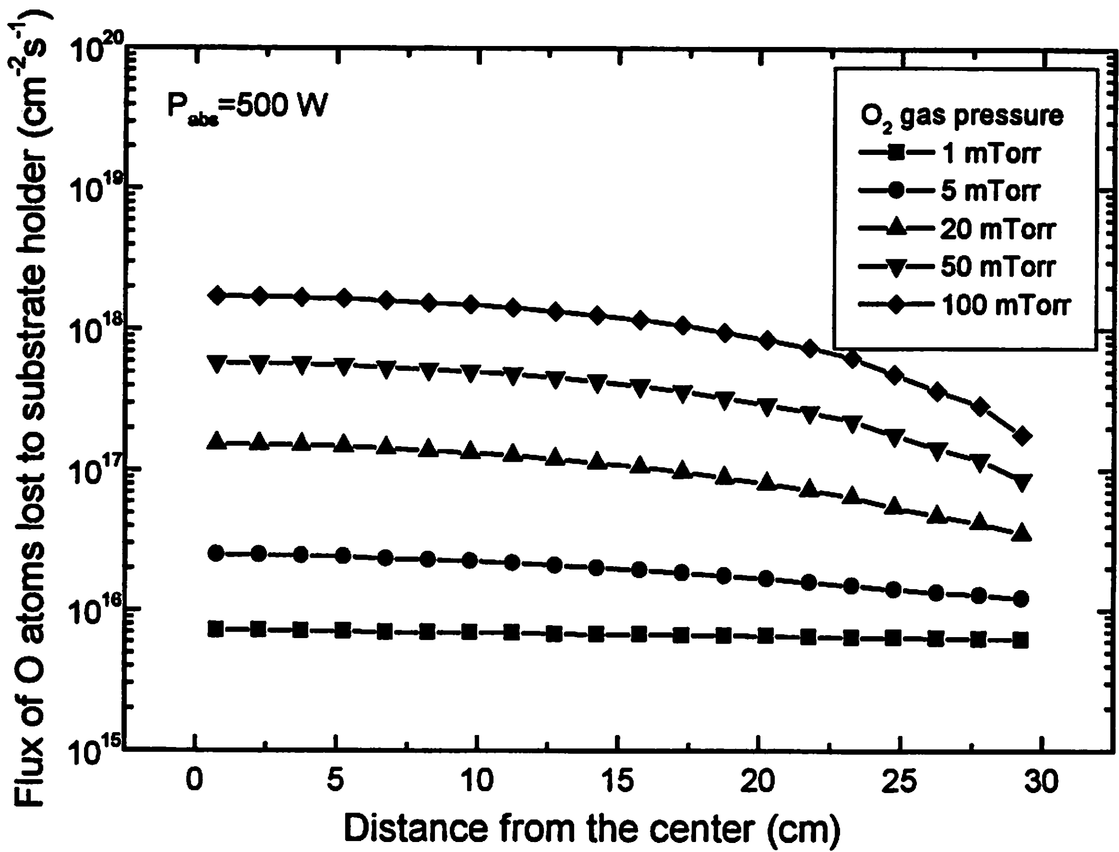

Fig. 18 The flux of O atoms lost to the substrate holder as a function of the distance from the center of the chamber.

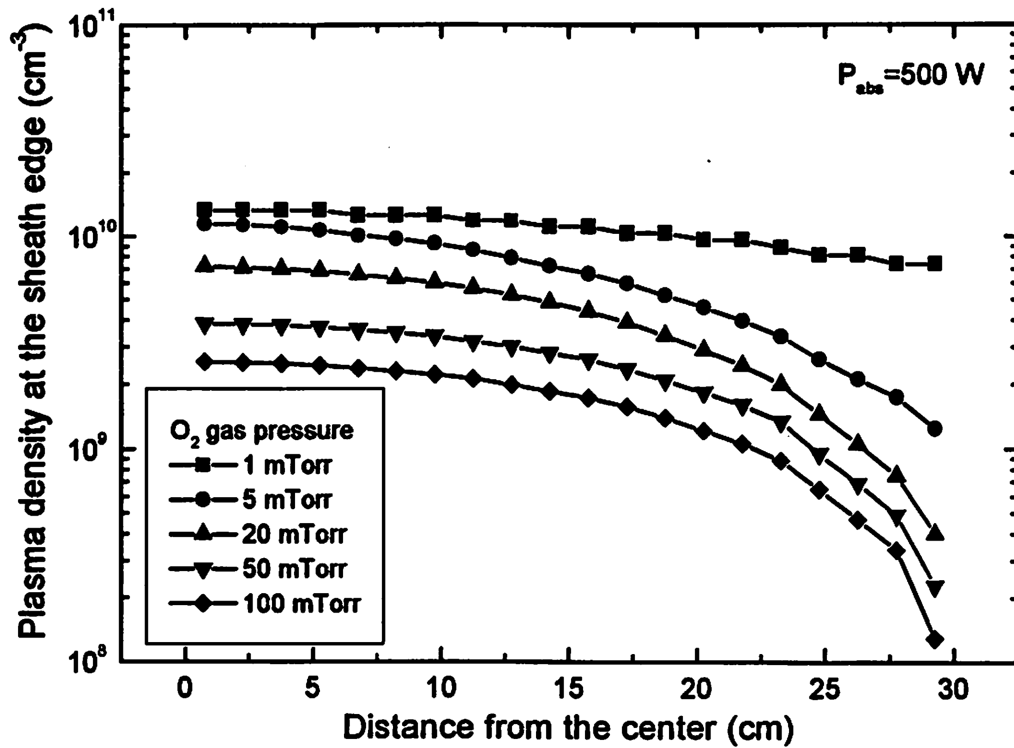

Fig. 19 Dependence of n_{is} on the distance from the center.

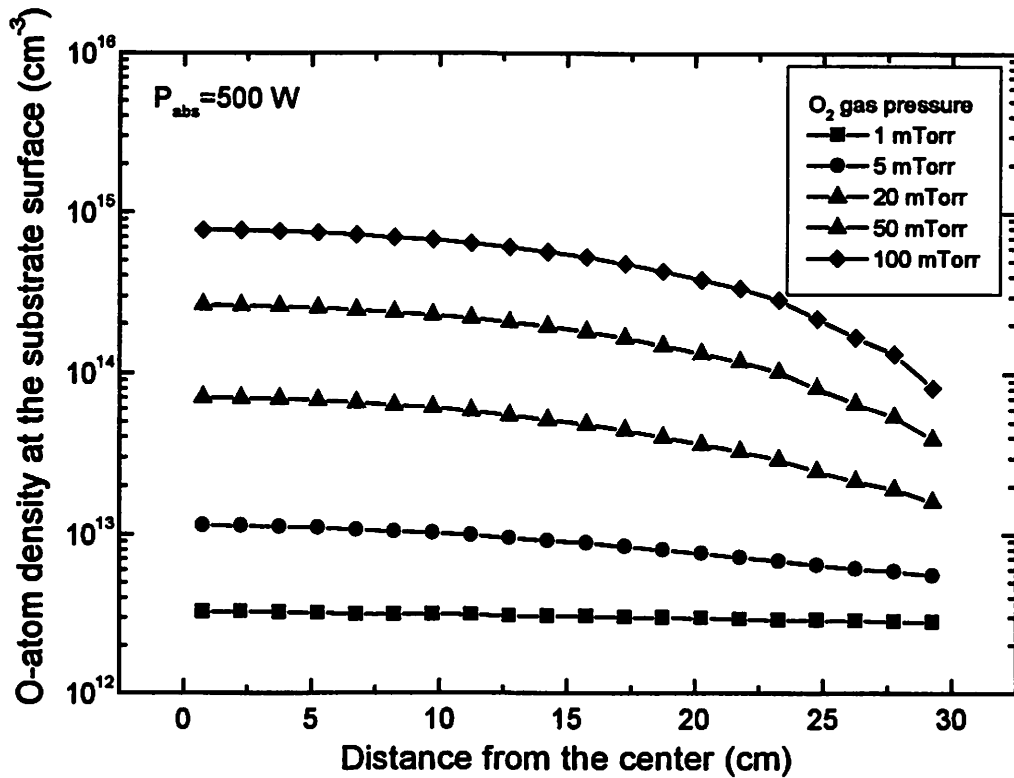

Fig. 20 Dependence of n_{Os} on the distance from the center.